

Resonant periodic orbits in the exoplanetary systems

K. I. Antoniadou, G. Voyatzis

Department of Physics, Aristotle University of Thessaloniki,
54124, Thessaloniki, Greece
kyant@auth.gr, voyatzis@auth.gr

June 28, 2021

The final publication is available at [springerlink.com](http://link.springer.com/article/10.1007/s10509-013-1679-8)
<http://link.springer.com/article/10.1007/s10509-013-1679-8>

Abstract

The planetary dynamics of $4/3$, $3/2$, $5/2$, $3/1$ and $4/1$ mean motion resonances is studied by using the model of the general three body problem in a rotating frame and by determining families of periodic orbits for each resonance. Both planar and spatial cases are examined. In the spatial problem, families of periodic orbits are obtained after analytical continuation of vertical critical orbits. The linear stability of orbits is also examined. Concerning initial conditions nearby stable periodic orbits, we obtain long-term planetary stability, while unstable orbits are associated with chaotic evolution that destabilizes the planetary system. Stable periodic orbits are of particular importance in planetary dynamics, since they can host real planetary systems. We found stable orbits up to 60° of mutual planetary inclination, but in most families, the stability does not exceed 20° - 30° , depending on the planetary mass ratio. Most of these orbits are very eccentric. Stable inclined circular orbits or orbits of low eccentricity were found in the $4/3$ and $5/2$ resonance, respectively.

keywords Extrasolar planets, general three body problem, mean motion resonances, periodic orbits, planetary systems.

1 Introduction

Over the last decades, there has been a tremendous increase of extrasolar planetary systems discoveries. Many of such systems consist of more than one planet and the study of planetary orbits concerning their long term stability is very interesting. Also, many planets seem to be locked in mean motion resonance (MMR), with the majority of which in 2/1 and by descending order, in 3/2, 5/2, 3/1, 4/1, 4/3, 5/1 and 7/2. However, the present estimation of their initial conditions may change significantly after obtaining additional observational data in the future.

Our study refers to the dynamics of a two-planet system locked in a MMR. Michtchenko et al. (2006) had studied the dynamics of many MMR in the planar case by extracting an appropriate averaged Hamiltonian and computing the families of its stationary points. Modeling a two-planet system with the general three body problem (GTBP), we can study the dynamics of the non-averaged system by computing families of periodic orbits in a suitable rotating frame (Voyatzis and Hadjidemetriou, 2005; Hadjidemetriou, 2006; Voyatzis, 2008; Voyatzis et al., 2009). These families of periodic orbits should coincide with the families of stationary points, provided that the averaged Hamiltonian is sufficiently correct. Also, it has been shown that families of periodic orbits can constitute paths that can drive the migration process and, consequently, trap the planets in a MMR (Lee and Peale, 2002; Ferraz-Mello et al., 2003; Hadjidemetriou and Voyatzis, 2010).

All of the above mentioned studies refer to the planar problem. In this paper, we, also, present new results for the planar case but we, mainly, focus on the dynamics of planetary orbits in space. The spatial GTBP, where planets have a mutual inclination, has been studied only for the 2/1 resonance in Antoniadou and Voyatzis (2013). We herewith determine families of symmetric periodic orbits in all possible configurations of the above mentioned resonances. We compute the spatial families by analytic continuation of vertical critical orbits (v.c.o.) of the planar general problem; a method introduced by Hénon (1973) for the restricted problem and extended to the general one by Ichtiaroglou and Michalodimitrakis (1980). Furthermore, we attempt to connect the linear stability of the periodic orbits with the long-term stability of planetary systems close to them.

The paper is organized as follows: In Sect. 2, we briefly present our model and the fundamental concepts of periodic orbits. In Sect. 3, we present the planar families of periodic orbits for different planetary mass ratios along with their horizontal stability and vertical critical orbits. In Sect. 4, we show the generated families of periodic orbits in space, with emphasis given on stable ones. In Sect. 5, we study the long term dynamical evolution of

orbits in the vicinity of periodic ones and conclude in Sect. 6.

2 The three dimensional GTBP, periodic orbits and stability

2.1 Equations of motion

We introduce a three dimensional system that consists of a Star, S , of mass m_0 and two inclined planets, P_1 and P_2 , of masses m_1 and m_2 , respectively, which are considered as point masses. The three bodies move in space $OXYZ$ (inertial frame) under their mutual gravitational attraction, where the origin O is their fixed center of mass and its Z -axis is parallel to the constant angular momentum vector, \mathbf{L} , of the system. The system is described by six degrees of freedom, which can be reduced by introducing a suitable rotating frame of reference, $Gxyz$, (Fig. 1) described in Michalodimitrakis (1979), such that:

1. Its origin coincides with the center of mass G of the bodies S and P_1 .
2. Its z -axis is always parallel to the Z -axis.
3. S and P_1 move always on xz -plane.

The Lagrangian of the system in the rotating frame of reference is:

$$\begin{aligned} \mathfrak{L} = \frac{1}{2}\mu[a(\dot{x}_1^2 + \dot{z}_1^2 + x_1^2\dot{\theta}^2) + b[(\dot{x}_2^2 + \dot{y}_2^2 + \dot{z}_2^2) \\ + \dot{\theta}^2(x_2^2 + y_2^2) + 2\dot{\theta}(x_2\dot{y}_2 - \dot{x}_2y_2)]] - V, \end{aligned} \quad (1)$$

where

$$\begin{aligned} V = -\frac{m_0m_1}{r_{01}} - \frac{m_0m_2}{r_{02}} - \frac{m_1m_2}{r_{12}}, \\ a = m_1/m_0, \quad b = m_2/m, \quad \mu = m_0 + m_1 \end{aligned}$$

and

$$\begin{aligned} r_{01}^2 &= (1 + a)^2(x_1^2 + z_1^2), \\ r_{02}^2 &= (ax_1 + x_2)^2 + y_2^2 + (az_1 + z_2)^2, \\ r_{12}^2 &= (x_1 - x_2)^2 + y_2^2 + (z_1 - z_2)^2. \end{aligned}$$

The Lagrangian of the system does not contain the angle between the axes OX and Gx , θ , therefore, the angular momentum $p_\theta = \partial\mathfrak{L}/\partial\dot{\theta}$ is constant and given by

$$p_\theta = \mu[ax_1^2\dot{\theta} + b[\dot{\theta}(x_2^2 + y_2^2) + (x_2\dot{y}_2 - \dot{x}_2y_2)]] = \text{const.} \quad (2)$$

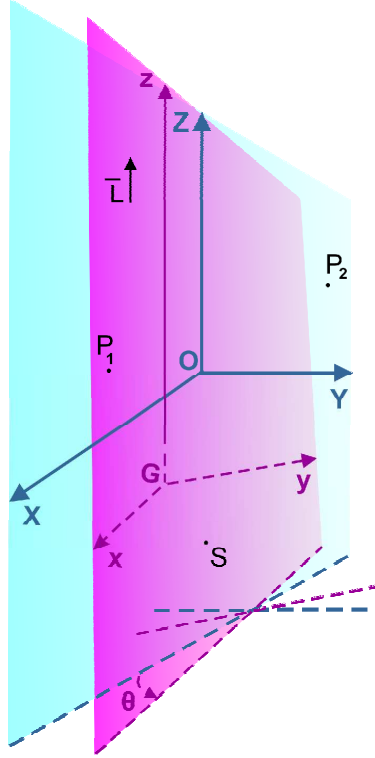


Figure 1: Inertial $OXYZ$ (blue) and rotating $Gxyz$ frame (magenta).

Due to the choice of the inertial system, concerning the components of the angular momentum \mathbf{L} , it always holds:

$$\begin{aligned}
 L_X &= \mu[b(y_2\dot{z}_2 - \dot{y}_2z_2) - \dot{\theta}(ax_1z_1 + bx_2z_2)] = 0, \\
 L_Y &= \mu[a(\dot{x}_1z_1 - x_1\dot{z}_1) + b(\dot{x}_2z_2 - x_2\dot{z}_2) \\
 &\quad - b\dot{\theta}y_2z_2] = 0, \\
 L_Z &= p_\theta.
 \end{aligned} \tag{3}$$

The above restrictions yield

$$\begin{aligned}
 z_1 &= \frac{b}{a} \left(\frac{y_2\dot{z}_2 - \dot{y}_2z_2}{x_1\dot{\theta}} - \frac{x_2z_2}{x_1} \right), \\
 \dot{z}_1 &= \frac{b}{ax_1} (\dot{x}_2z_2 - x_2\dot{z}_2 - \dot{\theta}y_2z_2) + \frac{\dot{x}_1}{x_1} z_1
 \end{aligned} \tag{4}$$

and

$$\dot{\theta} = \frac{p_\theta - b(x_2\dot{y}_2 - \dot{x}_2y_2)}{ax_1^2 + b(x_2^2 + y_2^2)}. \tag{5}$$

Thus, the independent variables in the rotating frame are only x_1 for the planet P_1 and x_2 , y_2 and z_2 for the planet P_2 and as a result, the system has been reduced to four degrees of freedom. The equations of motion are:

$$\begin{aligned}
\ddot{x}_1 &= -\frac{m_0 m_2 (x_1 - x_2)}{\mu r_{12}^3} - \frac{m_0 m_2 (a x_1 + x_2)}{\mu r_{02}^3} - \frac{\mu x_1}{r_{01}^3} + x_1 \dot{\theta}^2 \\
\ddot{x}_2 &= \frac{m m_1 (x_1 - x_2)}{\mu r_{12}^3} - \frac{m m_0 (a x_1 + x_2)}{\mu r_{02}^3} + x_2 \dot{\theta}^2 + 2 \dot{y}_2 \dot{\theta} + y_2 \ddot{\theta} \\
\ddot{y}_2 &= -\frac{m m_1 y_2}{\mu r_{12}^3} - \frac{m m_0 y_2}{\mu r_{02}^3} + y_2 \dot{\theta}^2 - 2 \dot{x}_2 \dot{\theta} - x_2 \ddot{\theta} \\
\ddot{z}_2 &= \frac{m m_1 (z_1 - z_2)}{\mu r_{12}^3} - \frac{m m_0 (a z_1 + z_2)}{\mu r_{02}^3}
\end{aligned} \tag{6}$$

The quantity $\ddot{\theta}$ is found by differentiating Eq. (5) with respect to time. We obtain

$$\ddot{\theta} = \frac{m_0 m_2}{\mu} \frac{y_2}{x_1} (r_{12}^{-3} - r_{02}^{-3}) - 2 \dot{\theta} \frac{\dot{x}_1}{x_1}. \tag{7}$$

2.2 Periodic orbits and analytic continuation in space

We consider the rotating frame $Gxyz$ and define the Poincaré section plane $\Pi = \{y_2 = 0, \dot{y}_2 > 0\}$. Then, the periodic orbits are defined as fixed or periodic points of this plane and provided that $y_2(0) = y_2(T)$, where T is the period, they satisfy the conditions:

$$\mathbf{q}(T) = \mathbf{q}_0 \tag{8}$$

where $\mathbf{q} = \{x_1, x_2, z_2, \dot{x}_1, \dot{x}_2, \dot{y}_2, \dot{z}_2\}$ and $\mathbf{q}_0 = \mathbf{q}(0)$. We note that for the planar problem is $z_2 = \dot{z}_2 = 0$, which implies that $z_1 = \dot{z}_1 = 0$, too. Due to the existence of the Jacobi integral, one of the above conditions is always fulfilled, when the rest ones are fulfilled.

If a periodic orbit has two perpendicular crossings with Π , it is *symmetric*. Next, we consider the symmetries with respect to the xz -plane and the x -axis (Michalodimitrakis, 1979). For a xz -symmetric periodic orbit the initial conditions are

$$\{x_{10}, x_{20}, z_{20}, \dot{y}_{20}\} \text{ and } \dot{x}_{10} = \dot{x}_{20} = \dot{z}_{20} = 0. \tag{9}$$

For a x -symmetric periodic orbit the initial conditions are

$$\{x_{10}, x_{20}, \dot{y}_{20}, \dot{z}_{20}\} \text{ and } \dot{x}_{10} = \dot{x}_{20} = z_{20} = 0. \tag{10}$$

Assuming a planar periodic orbit, we linearize the last of the Eq. (6) considering $z_{20} = \zeta_{10}$, $\dot{z}_{20} = \zeta_{20}$, with $|\zeta_{10}| \ll 1$ and we obtain the linear system (Ichtiaroglou et al., 1978)

$$\dot{\zeta}_1 = \zeta_2, \quad \dot{\zeta}_2 = A \zeta_1 + B \zeta_2 \tag{11}$$

where

$$\begin{aligned} A &= -\frac{mm_0}{\mu} [(1 - \gamma)d_{02}^{-3} + (a + \gamma)d_{12}^{-3}] \\ B &= -\frac{m_0m_2y_2}{\mu x_1\dot{\theta}} (d_{02}^{-3} - d_{12}^{-3}) \end{aligned} \quad (12)$$

with

$$d_{12}^2 = (x_1 - x_2)^2 + y_2^2, \quad d_{02}^2 = (ax_1 + x_2)^2 + y_2^2$$

and $\gamma = b \frac{x_2\dot{\theta} + \dot{y}_2}{x_1\dot{\theta}}$.

If $\Delta(T) = \{\xi_{ij}\}$, $i, j = 1, 2$, is the monodromy matrix of Eq. (11) for a planar periodic orbit of period T , we can define the *vertical stability index* (Hénon, 1973)

$$a_v = \frac{1}{2}(\xi_{11} + \xi_{22}) \quad (13)$$

If $|a_v| < 1$ or $|a_v| > 1$ the orbit is vertical stable or unstable, respectively. Any periodic orbit of the planar problem with $|a_v| = 1$ is *vertical critical*. A *vertical critical orbit* (v.c.o.) can be analytically continued in space. It is continued by varying the value of z_2 for the xz -symmetry or \dot{z}_2 for the x -symmetry (Ichtiaroglou et al., 1978).

2.3 Stability of 3D periodic orbits

The linear stability of periodic orbits is found by computing the eigenvalues of the 8×8 monodromy matrix of the variational equations of the system (6). Since the monodromy matrix is symplectic, we have 4 pairs of conjugate eigenvalues. We compute them by using the LAPACK routines of *Mathematica*. Iff all the eigenvalues lie on the unit circle, then the periodic orbit is *linearly stable*. Due to the existence of the energy integral, one pair of eigenvalues is equal to unity. The location of the other three pairs (see Fig. 2), may lead to simple, double, triple, complex or (as we call it here) *u*-complex instability (Marchal 1990; Skokos 2001).

In some cases, due to the limited accuracy, we cannot be sure whether an eigenvalue lies on the unit circle, or not. Therefore, apart from the computation of the eigenvalues we can estimate the evolution stability by using as index the Fast Lyapunov Indicator computed along the periodic orbit (Froeschlé et al. 1997; Voyatzis 2008).

2.4 Planetary resonant configurations and presentation of families of periodic orbits

Having assumed that $m_0 \gg m_{1,2}$ the periodic orbits in the rotating frame correspond to almost Keplerian ellipses described by the osculating orbital

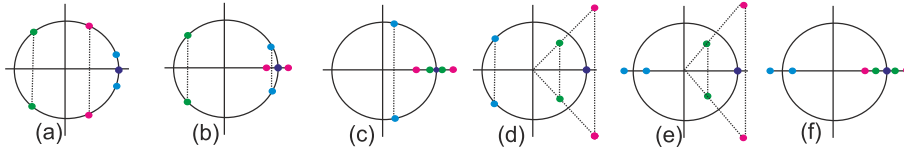


Figure 2: Stability types of 3D periodic orbits a) stability b) simple instability c) double instability d) complex instability e) u-complex instability f) triple instability.

elements a_i (semimajor axis), e_i (eccentricity), i_i (inclination), ω_i (argument of pericenter), Ω_i (longitude of ascending node) and λ_i (mean longitude). Throughout the present study we take $a_1 < a_2$ (thus, subscript 1 corresponds to the inner planet and 2 to the outer). The total mass of the system, m , is normalized to unity, i.e. $m = m_0 + m_1 + m_2 = 1$. The inner planet's mass is fixed to $m_J = 10^{-3}$ (Jupiter's mass), unless otherwise stated.

Mean motion resonances are associated with the non-circular families of periodic orbits for which $\frac{n_1}{n_2} \approx \frac{p+q}{p}$, where $q, p \neq 0$ are integers and n_i denotes the mean motion of the planet P_i . In this case, we can introduce the resonant angles

$$\begin{aligned}\theta_1 &= (p+q)\lambda_1 - p\lambda_2 - q\varpi_1 \\ \theta_2 &= (p+q)\lambda_1 - p\lambda_2 - q\varpi_2\end{aligned}\tag{14}$$

Also, we may refer to the apsidal difference $\Delta\varpi = \varpi_1 - \varpi_2$. For symmetric periodic orbits, we have $\Delta\varpi = 0$ (aligned planets) or $\Delta\varpi = \pi$ (antialigned planets). Also, we assume that at $t = 0$ the planets are placed at periastron, $M_i = 0$ or apoastron, $M_i = \pi$, where M_i indicates the mean anomaly of planet P_i . Thus, we get four resonant configurations and we can use the resonant angles (θ_1, θ_2) to distinct them. Therefore, the four configurations arising are $(0, 0)$, $(\pi, 0)$, (π, π) and $(0, \pi)$. However, for resonances with $q = \text{even}$, we always have, at $t = 0$, $\theta_1 - \theta_2 = q\Delta\varpi = 0$ and, consequently, the pair of angles (θ_1, θ_2) would not allow us to distinguish the different configurations. In such cases, e.g. the 3/1 resonance, where $q = 2$, we shall use the pair (θ_3, θ_1) , where the resonant angle θ_3 is defined as

$$\theta_3 = (p+q)\lambda_1 - p\lambda_2 - \frac{q}{2}(\varpi_1 + \varpi_2).\tag{15}$$

Following the literature (Michtchenko et al., 2006), we project the families of planar periodic orbits in the eccentricity plane (e_1, e_2) . In order to distinguish the families of different configurations in the projection plane we use both positive and negative values for the eccentricities. The positive values of e_i correspond to $\theta_i = 0$ and the negative ones to $\theta_i = \pi$.

Evidently, the periodic solutions generally depend on planetary masses. It has been shown by (Beaugé et al., 2003; Ferraz-Mello et al., 2006) that the families of periodic orbits on the projection plane (e_1, e_2) depend on the mass ratio of the planets, $\rho = \frac{m_2}{m_1}$ and not on planetary masses individually, provided that $m_i \ll m_0$. The various families belonging to the same configuration differ from one another in ρ , which usually extends in our computations from 0.01 to 20. The families of the same resonance and same configuration (but different ρ) form a *group* of families.

The v.c.o. of the families are classified according to the symmetry of the periodic orbits they generate: xz -symmetric and x -symmetric orbits are denoted with symbols \widehat{F} and \widehat{G} , respectively. They can be, also, classified according to the resonance, $\frac{p+q}{p}$ and the configuration (θ_1, θ_2) they belong to¹.

Concerning the spatial problem, we, also, have $\Delta\varpi = 0$ or π and $\theta_i = 0$ or π . Thus, the spatial families are denoted with symbols F and G , similarly to the v.c.o. where they start from. Also, the resonance and the configuration is indicated with a superscript and a subscript, respectively, i.e. we name the families as $F_{(\theta_1, \theta_2)}^{p+q/p}$ or $G_{(\theta_1, \theta_2)}^{p+q/p}$. In case there exist more than one groups of families or v.c.o. in the same configuration and resonance, symbols F and G are primed. We present the spatial families in the $3D$ projection space $(e_1, e_2, \Delta i)$, where Δi is the mutual inclination of the planets given by the cosine rule

$$\cos \Delta i = \cos i_1 \cos i_2 + \sin i_1 \sin i_2 \cos(\Omega_1 - \Omega_2).$$

We have computed the periodic orbits by solving numerically the equations (6) of the rotating frame using the Bulirsch-Stoer integrator and setting the minimum accuracy to 10^{-14} . The periodicity conditions (9) or (10) are satisfied at least up to 12 decimal digits after successive differential approximations. Since we aim to demonstrate a global view of stability and instability regions in phase space, we do not provide the accurate data of our computations. Instead, we present graphs of eccentricities and mutual inclination to which the estimated observational data can be assigned. The ratio of planetary semimajor axes can be approximated by the particular resonance, i.e. $\frac{a_1}{a_2} \approx \left(\frac{p+q}{p}\right)^{-2/3}$. We should remark that in extrasolar systems with very massive planets (e.g. $m_i \gtrsim 10 m_J$), the mean motion ratio may differ significantly from the rational value $(p+q)/p$.

¹We remind that for even values of q , we consider the pair (θ_3, θ_1) .

3 Planar families of symmetric periodic orbits

We herewith present families of symmetric planar periodic orbits in the MMRs 4/3, 3/2, 5/2, 3/1 and 4/1. We have computed the vertical stability of periodic orbits in each family and present the v.c.o. found. Stable v.c.o. are of particular importance, since they can yield, after continuation process, families of spatial stable orbits, where extrasolar planets could be trapped to.

We depict the characteristic curves of the families on the projection plane (e_1, e_2) . The segments of the families which consist of stable orbits are presented with bold blue lines, while the segments of unstable ones are depicted with red lines. The v.c.o. which generate xz -symmetric periodic orbits in space are presented by magenta-coloured dots, whereas the x -symmetric with green dots. Bold gray lines represent close encounters between the planets.

3.1 4/3 resonance

Extrasolar planetary systems close to 4/3 mean motion resonance are e.g. HD 200964 (Wittenmyer et al., 2012) and Kepler 29. In Fig. 3, we present the planar families of periodic orbits along with their stability and the v.c.o. they possess. There exists one group of families of periodic orbits that bifurcates from $(0, 0)$ (circular family) and starts as stable; it belongs to the configuration $(0, \pi)$. In the configuration $(\pi, 0)$, we obtain stable orbits above the collision line. This means that the planetary orbits intersect each other. However, due to the phase protection mechanism offered by the resonance, the planets avoid collisions and their orbits are stable. The same holds for the same configuration of all studied resonances.

In Table 1, we have classified the v.c.o. in accordance with the configuration to which they belong and the symmetry of spatial periodic orbits they generate. The configurations $(0, 0)$ and (π, π) do not have any v.c.o.. There are, also, circular v.c.o., at $(e_1, e_2) \approx (0, 0)$, which are not included in the Table. They exist for mass ratio values approximately in the interval $0.35 < \rho < 0.85$, and as we will see in Sect. 4.1, circular families of inclined orbits bifurcate from them.

3.2 3/2 resonance

The 3/2 mean motion resonance is apparent in many exosolar planetary systems, e.g. HD 45364 (Rein et al., 2010), KOI 55 (Callegari and Rodríguez,

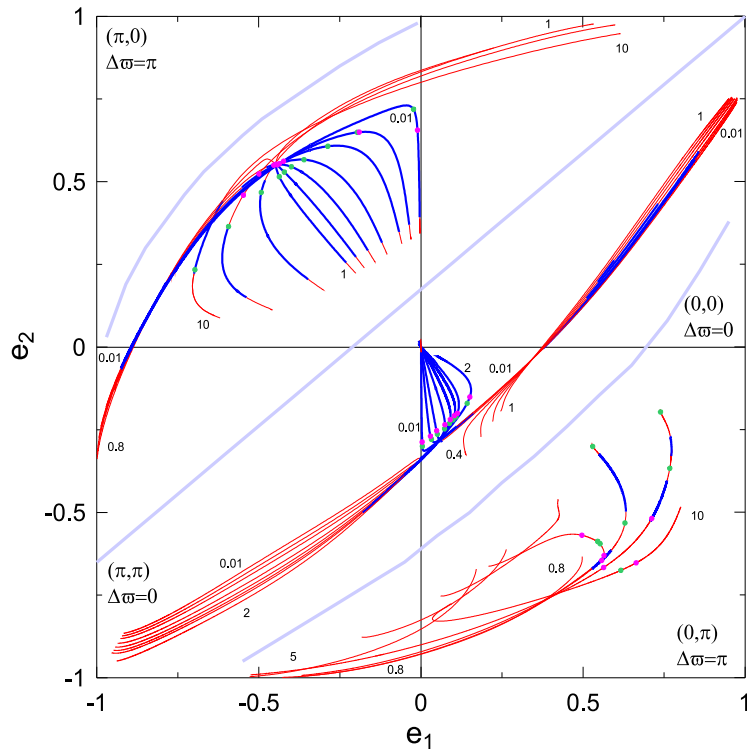


Figure 3: Planar families of symmetric periodic orbits in $4/3$ resonance for various (indicated) mass ratios. The particular configuration (θ_1, θ_2) for each quarter is indicated. Bold blue lines represent stable families, while the red ones the unstable families. Magenta or green coloured dots correspond to \widehat{F} and \widehat{G} v.c.o., respectively. The mass ratio ρ for some indicative families is given. Bold gray lines stand for close encounters between the planets.

Table 1: Eccentricity values of v.c.o. in 4/3 resonance.

ρ	$\widehat{F}_{(0,\pi)}^{4/3}$		$\widehat{G}_{(0,\pi)}^{4/3}$		$\widehat{F}_{(\pi,0)}^{4/3}$		$\widehat{G}_{(\pi,0)}^{4/3}$	
	e_1	e_2	e_1	e_2	e_1	e_2	e_1	e_2
0.01	0.003	0.287	0.004	0.299	0.010	0.655	0.022	0.719
0.1	0.029	0.269	0.032	0.278	0.190	0.649	0.196	0.649
0.2	0.048	0.253	0.050	0.263	0.423	0.561	0.287	0.607
0.4	0.073	0.234	0.072	0.247	0.437	0.554	0.360	0.566
0.6	0.090	0.219	0.087	0.230	0.442	0.551	0.399	0.545
0.8	0.103	0.207	0.098	0.219	0.446	0.551	0.421	0.529
	0.112	0.200	0.107	0.210	0.447	0.553	0.437	0.515
1	0.496	0.568	0.545	0.587				
	0.564	0.629	0.552	0.594				
	0.150	0.150	0.142	0.169	0.454	0.550	0.492	0.467
2	0.557	0.644	0.629	0.531				
			0.529	0.300				
5	0.563	0.666	0.767	0.366	0.547	0.459	0.593	0.364
	0.711	0.518	0.739	0.196	0.499	0.523		
10	0.663	0.652	0.616	0.675			0.697	0.233

2013), and a lot of Kepler systems (see Steffen et al. (2013, 2012)). In Fig. 4, we present 3/2 resonant families of periodic orbits and the v.c.o. they possess.

In configuration $(0, \pi)$, similarly to the 4/3 resonance, there is a group of families of stable periodic orbits that bifurcates from the circular family of periodic orbits. The configuration $(\pi, 0)$ has, also, families of periodic orbits with stable regions. The v.c.o. of these configurations are shown in Table 2. The configuration (π, π) does not have any v.c.o. and its families are totally unstable. The families in the configuration $(0, 0)$ have no v.c.o., too.

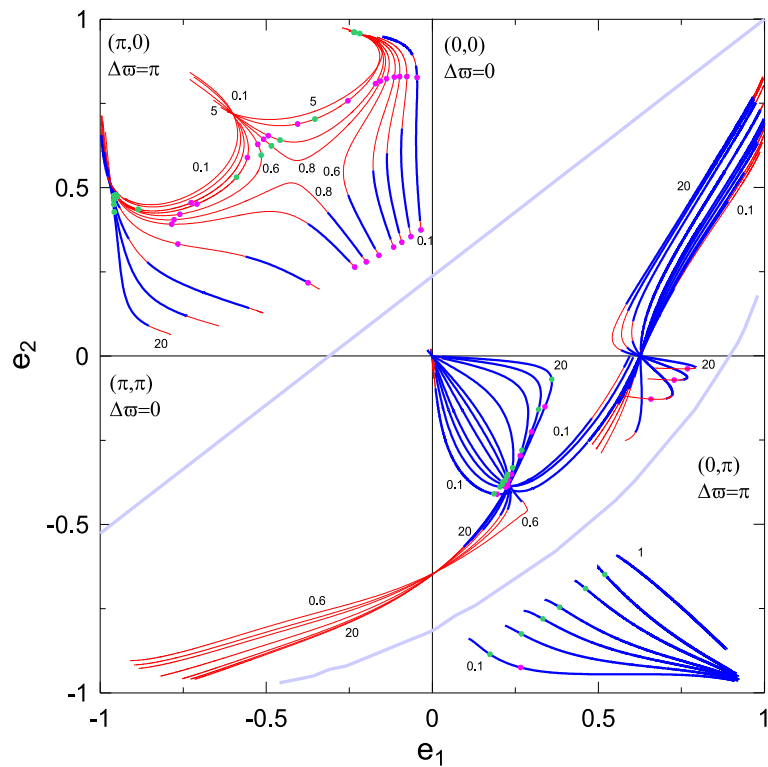


Figure 4: Planar families of symmetric periodic orbits in 3/2 resonance. They are presented as in Fig. 3.

3.3 5/2 resonance

The extrasolar planetary systems HD 1461 and HD 21693 are locked near the 5/2 resonance, while planets of the multiplanetary systems HD 10180 (f,e) (Lovis et al., 2011) and HD 181433(d,c) (Campanella, 2011; Campanella et al., 2013) seem to evolve in it. Particular families of periodic orbits of

Table 2: Eccentricity values of v.c.o. in 3/2 resonance.

ρ	$\widehat{F}_{(0,\pi)}^{3/2}$		$\widehat{G}_{(0,\pi)}^{3/2}$		$\widehat{F}_{(\pi,0)}^{3/2}$		$\widehat{G}_{(\pi,0)}^{3/2}$	
	e_1	e_2	e_1	e_2	e_1	e_2	e_1	e_2
0.1	0.195	0.409	0.185	0.408	0.034	0.374		
	0.266	0.924	0.173	0.885	0.045	0.826		
0.2	0.221	0.389	0.203	0.388	0.064	0.354		
			0.268	0.824	0.076	0.829		
0.3	0.227	0.384	0.211	0.380	0.091	0.337	0.885	0.435
			0.332	0.780	0.726	0.455		
0.4					0.098	0.829		
	0.225	0.381	0.211	0.374	0.116	0.323	0.589	0.530
0.4			0.383	0.745	0.114	0.828		
					0.708	0.451		
0.6					0.557	0.589		
	0.226	0.376	0.220	0.368	0.160	0.298	0.515	0.596
0.6			0.461	0.690	0.760	0.421	0.947	0.474
					0.525	0.628		
0.8					0.137	0.823		
	0.226	0.368	0.222	0.358	0.198	0.279	0.952	0.477
0.8			0.519	0.648	0.777	0.404	0.484	0.624
					0.508	0.643	0.236	0.961
1					0.156	0.816		
	0.229	0.367	0.226	0.350	0.233	0.264	0.954	0.477
1					0.784	0.391	0.458	0.641
					0.493	0.654	0.233	0.960
2					0.171	0.808		
	0.238	0.350	0.241	0.331	0.374	0.217	0.958	0.476
2					0.766	0.332	0.353	0.703
					0.405	0.688	0.218	0.957
5					0.254	0.757		
	0.264	0.295	0.269	0.279			0.959	0.462
10	0.658	0.127						
	0.298	0.224	0.320	0.158			0.959	0.450
20	0.728	0.071						
	0.339	0.150	0.359	0.069			0.957	0.428
	0.768	0.037						

this resonance were given by Psychoyos and Hadjidemetriou (2005). In Fig. 5, we present the structure of families of periodic orbits belonging to each configuration.

For each configuration we obtain families that bifurcate from circular orbits. At $(0,0)$ the picture is quite complicated and we added a magnification plot with few representative family curves. Segments of stability along the families are evident in every configuration. In Table 3, we show the v.c.o. of the configurations $(0,\pi)$ and $(\pi,0)$. The rest ones do not have any v.c.o..

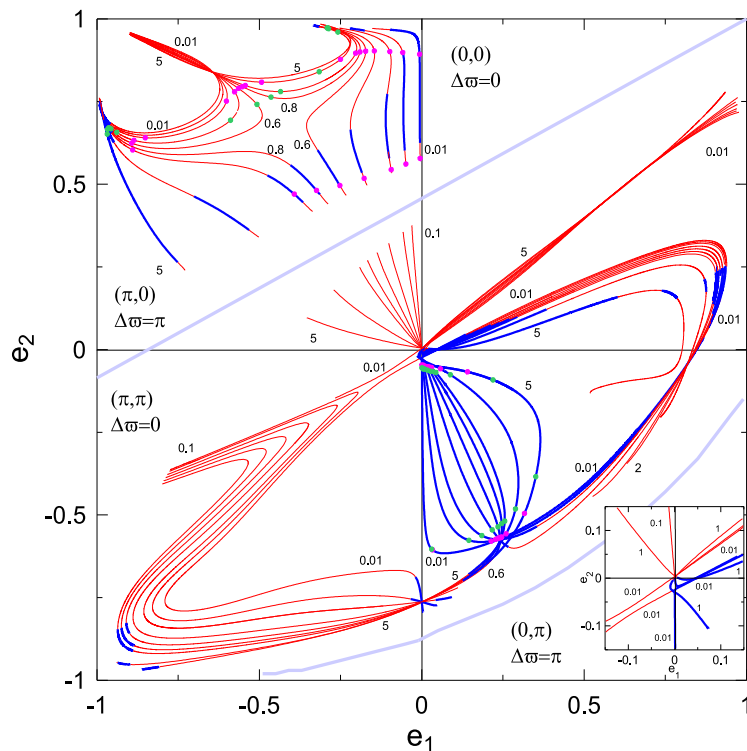


Figure 5: Presentation of planar families of symmetric periodic orbits in $5/2$ resonance, as in Fig. 3.

3.4 $3/1$ resonance

The $3/1$ resonance has been observed in the following planetary systems: HD 60532 (Laskar and Correia, 2009), HD 10180(e,d) (Lovis et al., 2011), and possibly in HD 20781 and HD 20003. The structure and stability of each group of families belonging to different configurations is thoroughly described

Table 3: Eccentricity values of v.c.o. in 5/2 resonance.

ρ	$\widehat{F}_{(0,\pi)}^{5/2}$		$\widehat{G}_{(0,\pi)}^{5/2}$		$\widehat{F}_{(\pi,0)}^{5/2}$		$\widehat{G}_{(\pi,0)}^{5/2}$	
	e_1	e_2	e_1	e_2	e_1	e_2	e_1	e_2
0.01	0.032	0.605	0.030	0.603	0.005	0.577		
	0.0003	0.046	0.0004	0.055	0.006	0.892		
0.1	0.213	0.579	0.145	0.576	0.048	0.560		
	0.003	0.047	0.004	0.058	0.058	0.897		
0.2	0.227	0.573	0.184	0.562	0.094	0.544		
	0.006	0.048	0.008	0.058	0.851	0.640		
					0.601	0.751		
					0.098	0.900		
0.4	0.235	0.569	0.216	0.545	0.177	0.517	0.938	0.656
	0.013	0.051	0.017	0.062	0.886	0.632	0.588	0.693
					0.576	0.779		
					0.146	0.902		
0.6	0.240	0.569	0.234	0.535	0.252	0.495	0.956	0.667
	0.018	0.051	0.026	0.065	0.892	0.624	0.507	0.741
					0.564	0.789	0.291	0.973
					0.172	0.902		
0.8	0.243	0.567	0.246	0.525	0.892	0.614	0.962	0.669
	0.024	0.052	0.034	0.066	0.324	0.481	0.464	0.763
					0.552	0.794	0.289	0.971
					0.190	0.899		
1	0.246	0.566	0.255	0.518	0.392	0.469	0.964	0.670
	0.030	0.054	0.043	0.069	0.890	0.603	0.434	0.780
					0.543	0.798	0.286	0.970
					0.203	0.896		
2	0.259	0.556	0.288	0.481	0.493	0.808	0.967	0.665
	0.057	0.057	0.088	0.076	0.250	0.877	0.315	0.840
							0.258	0.960
5	0.316	0.495	0.351	0.384			0.968	0.651
	0.141	0.067	0.219	0.091				

in Voyatzis (2008) and following this study, we kept the inner planet’s mass fixed to $8 \cdot 10^{-4}$. Furthermore, in Fig. 6, we show the v.c.o. of each family.

In configuration $(0, \pi)$ there are couples of x - symmetric v.c.o. from which, as we shall see in Sect. 4.4, one family bifurcates forming a bridge from one v.c.o. to the other for mass ratios $\rho < 0.158$. V.c.o. of such symmetry appear again for $e_1 > 0.75$. From the rest v.c.o. xz -symmetric periodic orbits bifurcate. We note that this behaviour was, also, reported in the study of 2/1 resonance (Antoniadou and Voyatzis (2013)). Stable v.c.o., also, appear in configuration $(\pi, 0)$. All of them are given in Table 4.

The configuration $(0, 0)$ has many v.c.o. that belong to unstable families of periodic orbits. However, we should state the bifurcations that take place as ρ increases, in order to show the complexity of the dynamics: i) For $\rho < 0.02375$ there exists one \widehat{G} v.c.o. (i.e. of x -symmetry) in each family (green dots). ii) For $0.025 < \rho < 0.105$ there are couples of \widehat{G} v.c.o. (black dots). iii) For $0.11 < \rho < 0.14375$ there is no v.c.o. iv) For $0.15 < \rho < 1.875$ there appears a \widehat{F} v.c.o., from which xz -symmetric spatial periodic orbits bifurcate (gray dots). v) For $1.9 < \rho < 13.5$ there are no v.c.o. vi) For $13.5 < \rho < 20$ there is again one \widehat{G} v.c.o. of consequent x -symmetry (green dots).

Table 4: Eccentricity values of v.c.o. in 3/1 resonance.

ρ	$\widehat{F}_{(\pi,0)}^{3/1}$		$\widehat{G}_{(\pi,0)}^{3/1}$		$\widehat{F}_{(0,\pi)}^{3/1}$		$\widehat{G}_{(0,\pi)}^{3/1}$	
	e_1	e_2	e_1	e_2	e_1	e_2	e_1	e_2
					0.087	0.170	0.019	0.105
0.025							0.753	0.212
0.1	0.047	0.589			0.494	0.191	0.158	0.171
							0.693	0.203
0.25					0.595	0.192		
0.5	0.201	0.550			0.637	0.191	0.888	0.252
1	0.341	0.530			0.661	0.187	0.860	0.243
2	0.525	0.513	0.390	0.322	0.672	0.177	0.851	0.243
5	0.760	0.532	0.570	0.236	0.671	0.151	0.850	0.254
10	0.864	0.548	0.679	0.184	0.661	0.119	0.854	0.270
20	0.919	0.554			0.645	0.079	0.859	0.290

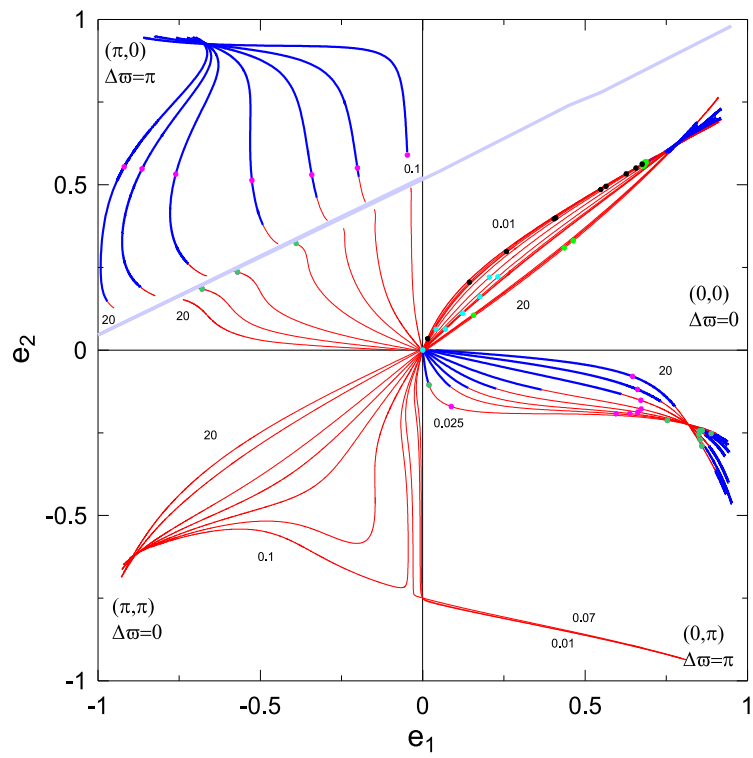


Figure 6: Presentation of planar families of symmetric periodic orbits in 3/1 resonance, as in Fig. 3.

3.5 4/1 resonance

Extrasolar planetary systems, which are trapped in 4/1 resonance, are e.g. HD 102272 (Niedzielski et al., 2009), HD 108874 (Goździewski et al., 2006; Libert and Henrard, 2007) and GJ 667C (Anglada-Escudé et al., 2012). In Figure 7, we depict the families, indicating the stability and the v.c.o. at each configuration.

Similarly to the 3/1 resonance, every configuration seems to have families that bifurcate from circular periodic orbits. Segments with stable orbits are apparent in every configuration, but only for the cases $(0,0)$ and $(0,\pi)$ we observe stability at nearly circular orbits. There are stable v.c.o. in configurations $(0,\pi)$ and $(\pi,0)$ and they are given in Table 5. In configuration $(0,0)$ all v.c.o are unstable, while in (π,π) they do not exist.

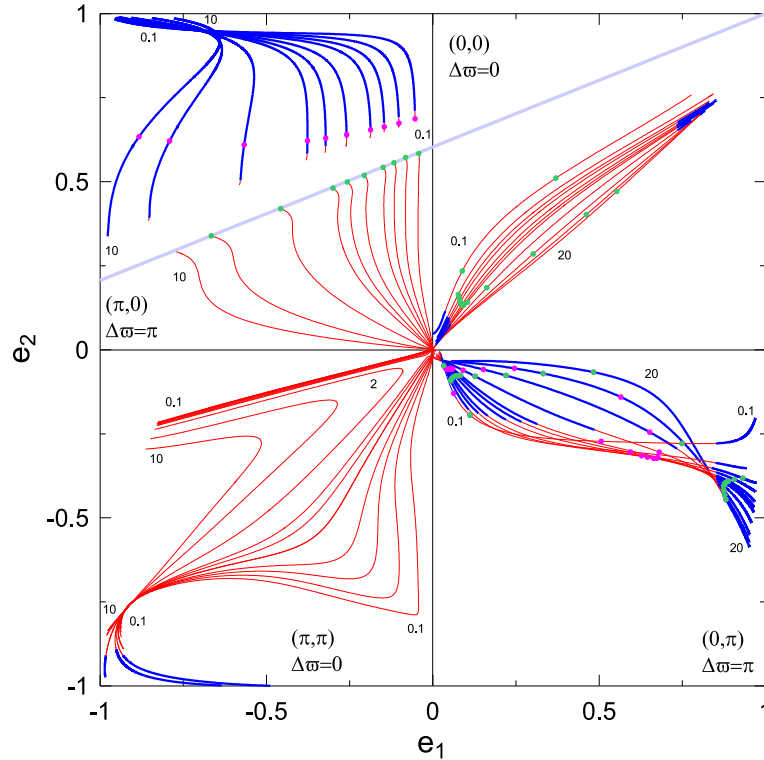


Figure 7: Presentation of planar families of symmetric periodic orbits in 4/1 resonance, as in Figure 3.

Table 5: Eccentricity values of v.c.o. in 4/1 resonance.

ρ	$\widehat{F}_{(0,\pi)}^{4/1}$		$\widehat{G}_{(0,\pi)}^{4/1}$		$\widehat{F}_{(\pi,0)}^{4/1}$		$\widehat{G}_{(\pi,0)}^{4/1}$	
	e_1	e_2	e_1	e_2	e_1	e_2	e_1	e_2
0.1	0.032	0.046	0.062	0.129	0.053	0.686	0.042	0.583
	0.506	0.272	0.111	0.194				
			0.748	0.278				
0.2	0.037	0.054	0.054	0.092	0.101	0.674	0.081	0.571
	0.593	0.304						
0.3	0.042	0.058	0.057	0.085	0.146	0.663	0.116	0.556
	0.627	0.314	0.931	0.382				
0.4	0.045	0.057	0.061	0.081	0.186	0.653	0.149	0.542
	0.644	0.319	0.906	0.385				
0.6	0.050	0.056	0.068	0.077	0.259	0.639	0.206	0.518
	0.663	0.322	0.888	0.390				
0.8	0.056	0.058	0.076	0.076	0.321	0.629	0.257	0.499
	0.672	0.322	0.881	0.393				
1	0.059	0.056	0.083	0.076	0.376	0.621	0.300	0.480
	0.676	0.320	0.878	0.396				
2	0.090	0.060	0.126	0.078	0.567	0.609	0.457	0.419
	0.680	0.304	0.873	0.404				
5	0.151	0.058	0.219	0.076	0.791	0.621	0.665	0.338
	0.651	0.245	0.874	0.418				
10	0.245	0.055	0.331	0.070	0.883	0.633		
	0.565	0.140	0.877	0.431				
20			0.483	0.066				
			0.881	0.445				

4 Spatial families of periodic orbits

We herein present some indicative spatial families of periodic orbits, which bifurcate from stable v.c.o.. Such spatial families can start as stable or unstable. But families which bifurcate from an unstable v.c.o. start always as unstable. Of course, the stability type can change along the family. Along the continuation in the third dimension the symmetry does not change, but their starting configuration (θ_1, θ_2) of the planar v.c.o. may change along the spatial family. We remark that a family is named after the configuration of the v.c.o. it started from and it is presented in the projection space $(e_1, e_2, \Delta i)$ (see Sect. 2.4).

4.1 4/3 resonance

In Figure 8, we present families of 3D periodic orbits bifurcating from stable v.c.o. of the particular resonance. The configuration of these v.c.o. is $(0, \pi)$ or $(\pi, 0)$ and we obtain spatial families F and G (symmetries xz and x , respectively). We observe that in the projection space the families start with an increasing mutual inclination Δi , while the eccentricities do not vary significantly. This feature appears in most cases. For larger values of Δi , eccentricities may also vary significantly along the families.

In Figure 9, we depict the spatial families of periodic orbits that are continued from the circular v.c.o. (see Sect. 3.1) and we denote them with a prime. The $G'_{(0,\pi)^{4/3}}$ families are unstable, whilst the $F'_{(0,\pi)^{4/3}}$ families are stable up to a mutual inclination of 28° and 35° for mass ratios $\rho = 0.4$ and $\rho = 0.6$, respectively. But, for $\rho = 0.8$, $F'_{(0,\pi)^{4/3}}$ becomes totally unstable. Along the stable segments the eccentricities do not vary significantly and the planetary orbits remain almost circular. This is the only case of circular inclined periodic orbits we found.

In Figure 10, we show the maximum value of mutual inclination up to which stable orbits exist as a function of the mass ratio, ρ . We consider the cases where the families start having stable regions. We observe that the maximum mutual inclination of all the symmetries has the same behaviour, namely it reaches a maximum value (48° , 5° , 38° , corresponding to Figs. 8a,b,d, accordingly) and then, it decreases monotonically down to zero.

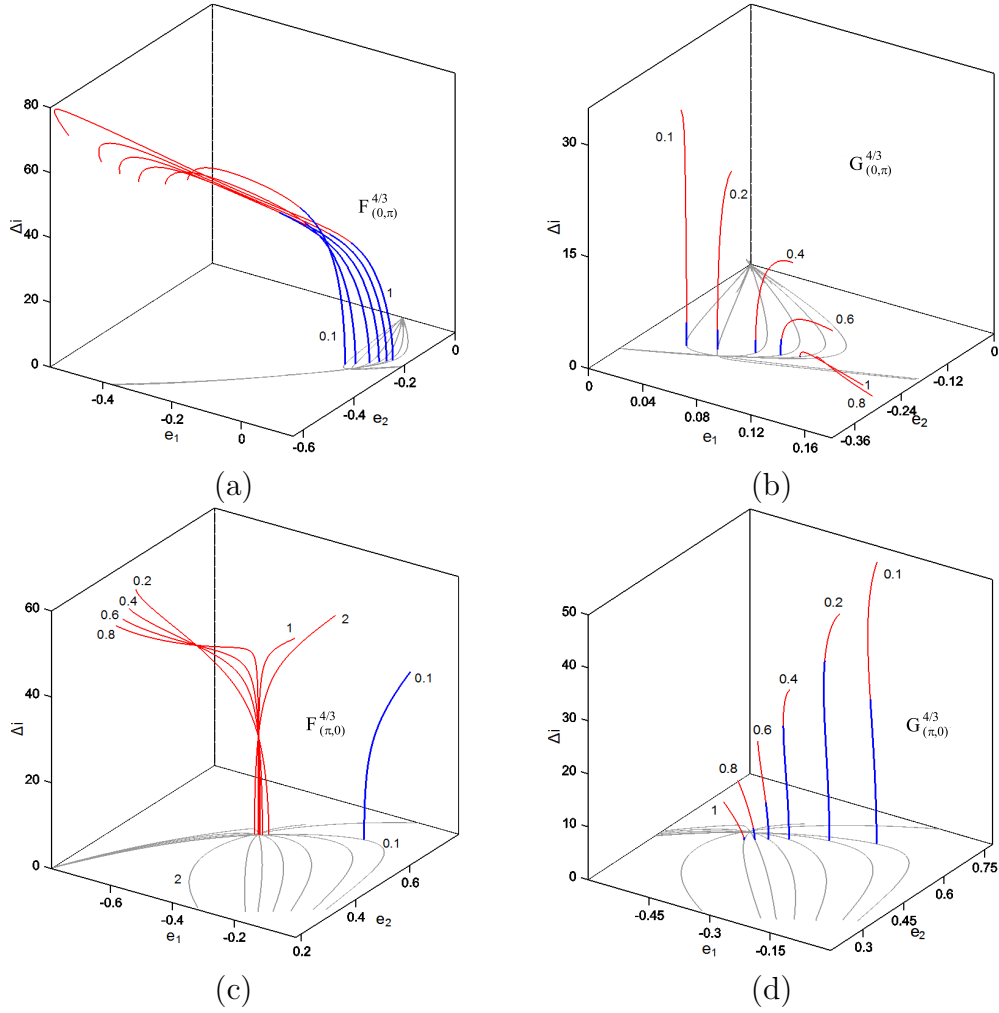


Figure 8: Spatial families of symmetric periodic orbits in $4/3$ resonance for the indicated mass ratios. Both configurations $(0, \pi)$ and $(\pi, 0)$ have xz -symmetric (panels **a,c**) and x -symmetric (panels **b,d**) families of periodic orbits. Blue and red coloured lines stand for stable and unstable orbits, respectively. The planar families, where they bifurcate from, are also presented with gray colour.

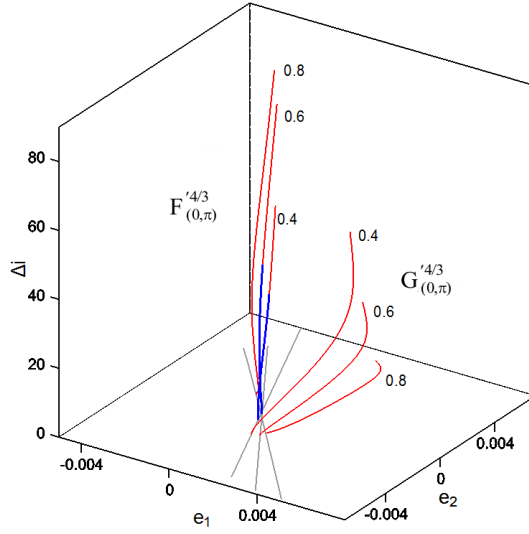


Figure 9: Spatial families of periodic that bifurcate from circular v.c.o. close to the 4/3 resonance.

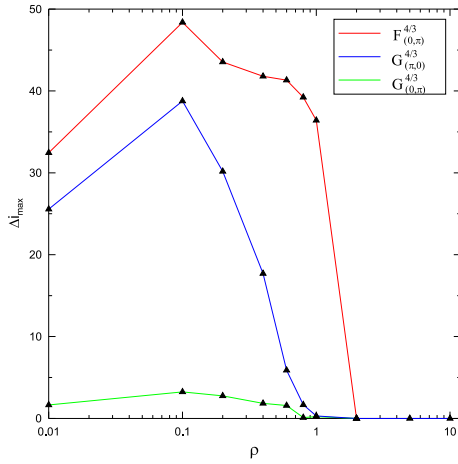


Figure 10: Maximum values of mutual inclination, Δi_{max} , up to which we obtain stable periodic orbits along the indicated families as a function of the mass ratio ρ .

4.2 3/2 resonance

In Fig. 11, we present the spatial groups of families of periodic orbits that belong to the configuration $(0, \pi)$. In panels **a** and **b**, the $F_{(0,\pi)}^{3/2}$ and $G_{(0,\pi)}^{3/2}$

families of periodic orbits are depicted. In panel **c**, we present a second group, $G'_{(0,\pi)}{}^{3/2}$, of x -symmetry families emerging from the group of planar families "above" the collision line (see Fig. 4). All of them start having stable regions, but the stability does not exceed the value $\Delta i \approx 1^\circ$. In panel **d**, we observe that the stability of families $F'_{(0,\pi)}{}^{3/2}$ appears up to a mutual inclination value Δi_{max} , which increases as ρ increases and reaches the value of 41° for $\rho = 20$. The families $G'_{(0,\pi)}{}^{3/2}$ show stability up to large mutual inclination values for $\rho > 1$ and for $\rho = 0.1$ where $\Delta i_{max} = 24^\circ$. As we mentioned above, the families $G'_{(0,\pi)}{}^{3/2}$ are, practically, totally unstable.

4.3 5/2 resonance

In Fig. 12a, we present the $G_{(0,\pi)}{}^{5/2}$ and $G'_{(0,\pi)}{}^{5/2}$ families of periodic orbits generated from the two pairs of v.c.o. of the planar families (see Sect. 3.3). We observe that $G_{(0,\pi)}{}^{5/2}$ consist of stable periodic orbits, while $G'_{(0,\pi)}{}^{5/2}$ are totally unstable. The maximum value of mutual inclination that the planets of the stable orbits reach is of 55° (see Fig. 12d, blue line). However, for $\rho \approx 1$, the stability is evident only for very small mutual inclination values.

In panels **b** and **c** of Fig. 12, we show the families $F_{(0,\pi)}{}^{5/2}$ and $F'_{(0,\pi)}{}^{5/2}$, respectively. For $\rho < 2$ families $F_{(0,\pi)}{}^{5/2}$ are stable up to large inclination values (up to 45° for $\rho = 0.4$). In their stable segments the eccentricities are almost constant. Families $F'_{(0,\pi)}{}^{5/2}$ start as stable, but their stability does not exceed 12° (for $\rho = 1$). The maximum mutual inclination value for each mass ratio is shown in panel **d**.

4.4 3/1 resonance

In Fig. 13, we present groups of the spatial families $F_{(\pi,0)}{}^{3/1}$ and $F'_{(0,\pi)}{}^{3/1}$ (panels **a** and **b**, respectively), for various mass ratios. In Fig. 14, we show the Δi_{max} which is reached by the orbits of the families $F_{(\pi,0)}{}^{3/1}$ as the planetary mass ratio ρ varies. For, approximately, $\rho < 0.5$ and $\rho \geq 10$ the families have no stable orbits. The highest value of Δi_{max} is obtained for $\rho = 5$ and is equal to 39° . For the families $F'_{(0,\pi)}{}^{3/1}$ we found that they are totally unstable for $\rho \leq 5$, but for $\rho \geq 10$ we obtain stability up to mutual inclination of approximately 50° .

An interesting characteristic curve is shown for the family $G'_{(0,\pi)}{}^{3/1}$ (Fig. 15). It starts and ends at the planar family (existence of couple of v.c.o.) and along its way, partially it follows a path with almost circular inclined orbits that extends in the interval $15^\circ < \Delta i < 72^\circ$. All orbits along this

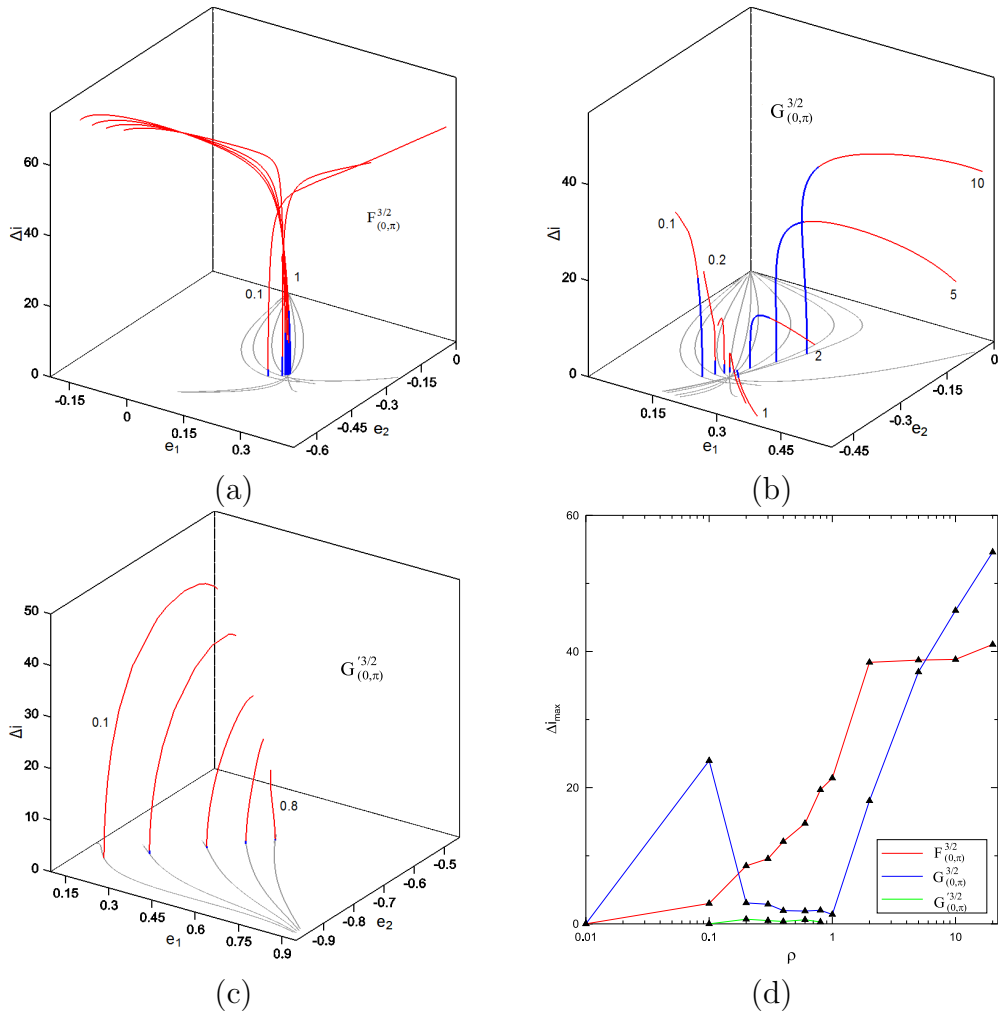


Figure 11: Spatial families of symmetric periodic orbits in 3/2 resonance for various mass ratios. **a** $F_{(0,\pi)}^{3/2}$, **b** $G_{(0,\pi)}^{3/2}$ and **c** $G_{(0,\pi)}'^{3/2}$ families of periodic orbits. **d** Maximum values of mutual inclination reached along the families as a function of the mass ratio ρ .

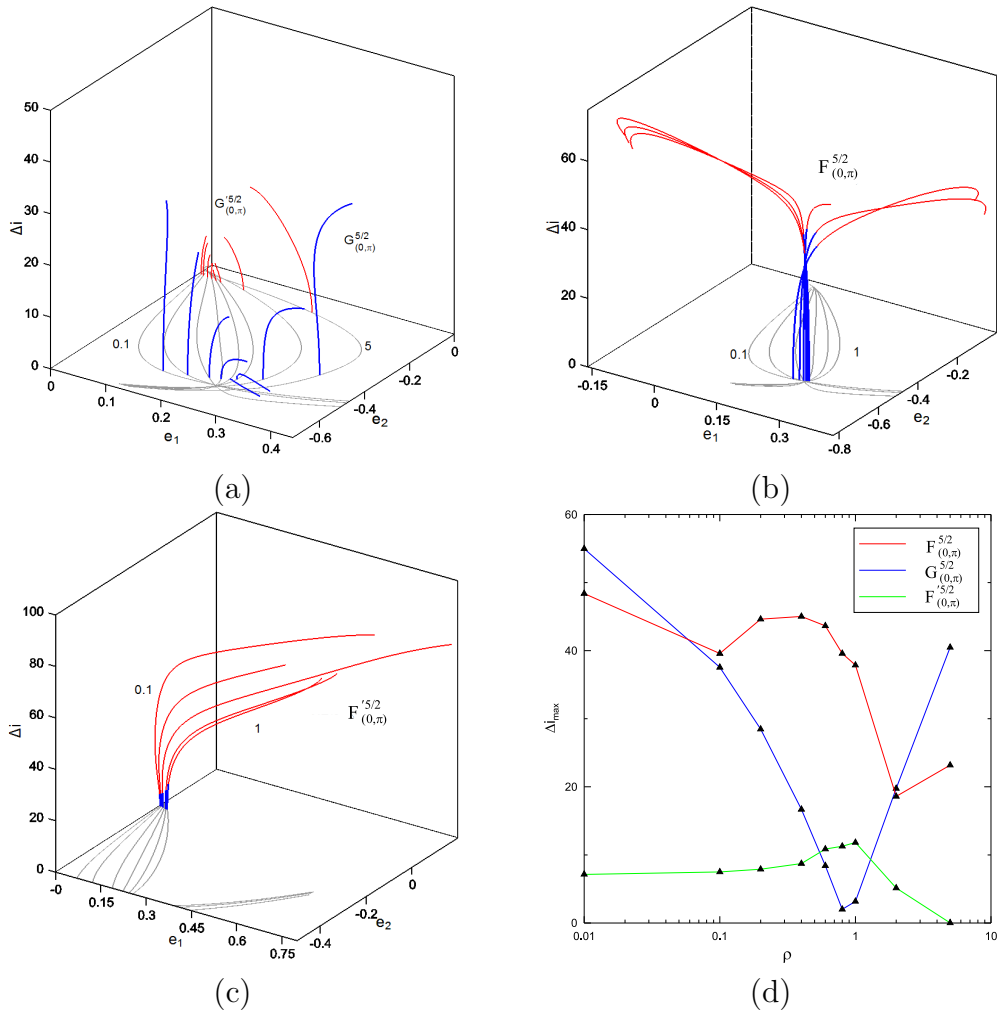


Figure 12: **a** Families $G_{(0,\pi)}^{5/2}$ **b** Families $F_{(0,\pi)}^{5/2}$ **c** Families $F_{(0,\pi)}^{5/2}$ **d** Maximum values of mutual inclination reached along the families as a function of the mass ratio ρ .

family are unstable.

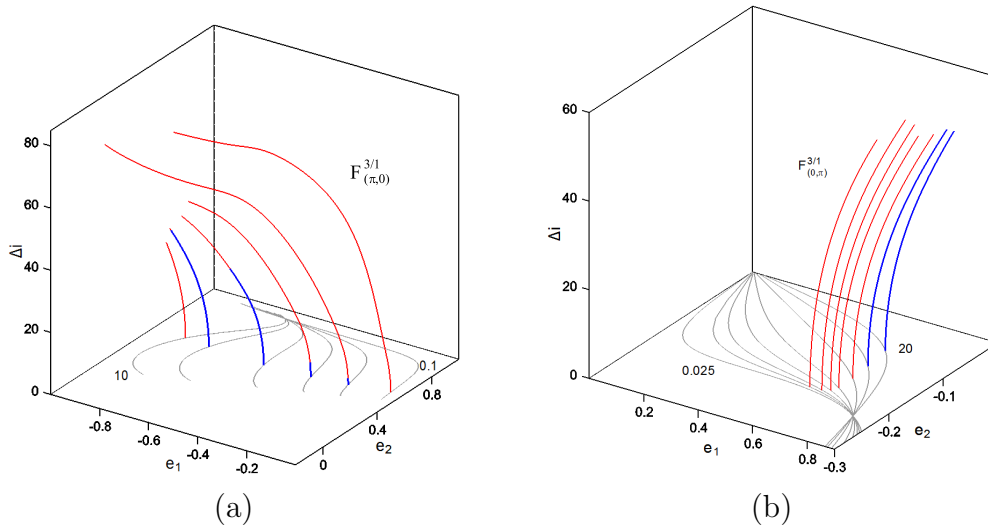


Figure 13: **a** Families $F_{(\pi,0)}^{3/1}$ and **b** $F_{(0,\pi)}^{3/1}$.

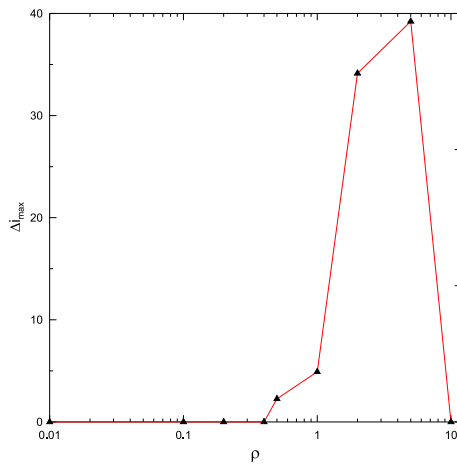


Figure 14: Maximum values of mutual inclination along the family $F_{(\pi,0)}^{3/1}$ as a function of the mass ratio ρ .

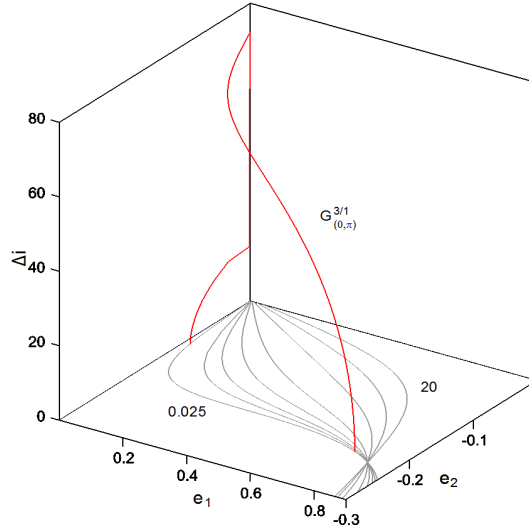


Figure 15: The $G_{(0,\pi)}^{3/1}$ family for $\rho = 0.025$. The segment for $15^\circ < \Delta i < 72^\circ$ consists of circular orbits.

4.5 4/1 resonance

In Fig. 16a, we present the spatial families of 4/1 resonance $F_{(0,\pi)}^{4/1}$ and $F'_{(0,\pi)}^{4/1}$. The first ones start having stable orbits for $\rho > 0.1$. The stable orbits extend up to a maximum mutual inclination value, which depends on ρ , as it is shown in Fig. 16d (red line). The families $F'_{(0,\pi)}^{4/1}$, although some of them ($5 \leq \rho \leq 10$) bifurcate from stable v.c.o., consist of unstable orbits. In Fig. 16b, the x -symmetric families $G_{(0,\pi)}^{4/1}$ and $G'_{(0,\pi)}^{4/1}$ are presented. $G'_{(0,\pi)}^{4/1}$ are unstable, while families $G_{(0,\pi)}^{4/1}$ always start as stable, but in the interval $0.6 < \rho < 0.8$ stability keeps only for $\Delta i < 0.5^\circ$ (Fig. 16d, blue line). There are also couples of v.c.o. from which the bifurcated families of x -symmetric periodic orbits start and end at them forming a bridge. They exist for mass ratios $\rho < 0.163$ and are totally unstable; they are not depicted.

In Fig. 16c, we show the families $F_{(\pi,0)}^{4/1}$, which start having stable segments for up to the mass ratio we computed them, i.e. $\rho \leq 5$. Also, in this case we obtain stable orbits of high mutual inclination, up to 47° at $\rho = 2$. We note that the particular v.c.o. correspond to crossing planetary orbits as it happens for any resonance in the configuration $(\pi, 0)$.

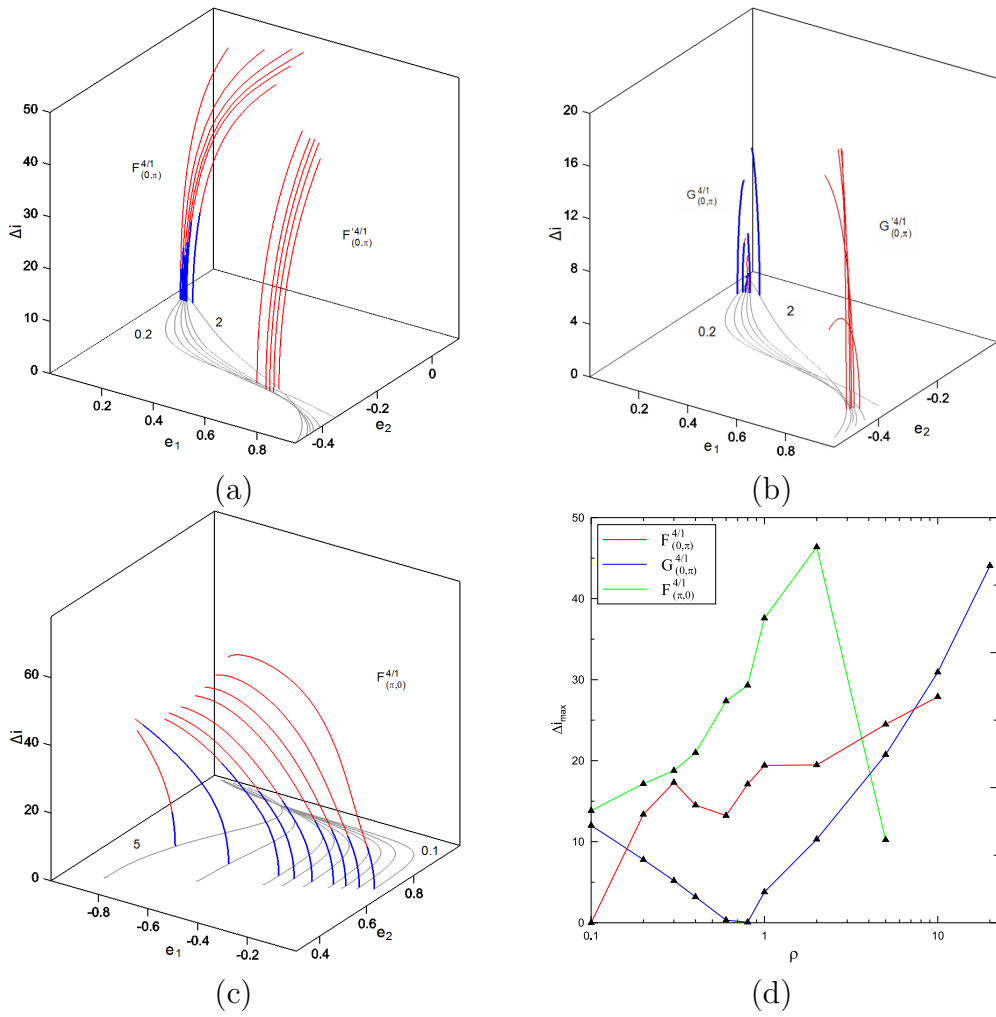


Figure 16: Spatial families of symmetric periodic orbits 4/1 resonance for various mass ratios. **a** $F_{(0,\pi)}^{4/1}$ **b** $G_{(0,\pi)}^{4/1}$ and **c** $F_{(\pi,0)}^{4/1}$ families. **d** Maximum values of mutual inclination reached along the families as a function of the mass ratio ρ .

5 Long-term dynamical evolution of orbits

It is known, that in Hamiltonian systems the stable periodic orbits are surrounded in phase space by invariant tori, where the motion is regular and bounded in the vicinity of them. Therefore, in these regions, as numerical simulations indicate, the long-term stability is guaranteed. In contrary, around unstable periodic orbits in the phase space chaotic regions exists. If chaos is weak, the planetary orbits evolve showing some irregularity in the oscillations of orbital elements, but the configuration of the system does not change significantly for long time intervals. However, in strongly chaotic regions the planetary system is destabilized and the planets show collisions or escapes.

We hereafter present some numerical results and attempt to connect the above mentioned behaviour of periodic orbits with the long-term dynamical evolution of spatial periodic orbits. We consider initial conditions from an unstable and a stable periodic orbit of the families $F_{(0,\pi)}^{5/2}$ for $\rho = 0.4$. During numerical integrations the relative error in energy and angular momentum is less than 10^{-11} (except in cases of close encounters). The regular or chaotic nature of the system's evolution can be also verified by the F.L.I. mentioned in Sect. 2.3.

5.1 Case i: Long-term evolution of a 3D unstable orbit

We consider the computed (with accuracy 10^{-12}) initial conditions of an unstable periodic orbit (from the family mentioned above) that correspond approximately to the orbital elements

$$\begin{aligned} a_1 &= 1.61, & e_1 &= 0.27, & i_1 &= 15.96^\circ, & \Omega_1 &= 90^\circ, & \omega_1 &= 270^\circ, & M_1 &= 0^\circ \\ a_2 &= 2.97, & e_2 &= 0.55, & i_2 &= 35.83^\circ, & \Omega_2 &= 270^\circ, & \omega_2 &= 270^\circ, & M_2 &= 180^\circ \end{aligned} \tag{16}$$

In Fig. 17, we depict the evolution of the orbital elements a_i , e_i and i_i and the resonant angles θ_1 , $\Delta\varpi$ and $\Delta\Omega$. Initially, the evolution takes place close to the unstable periodic orbit. The orbital elements remain almost constant and the resonant angles, θ_1 , $\Delta\varpi$ and $\Delta\Omega$, librate slightly around 0° , 180° and 180° , respectively, until 2×10^5 t.u.. However, due to the instability (and since the initial conditions do not correspond exactly to the periodic orbit), the evolution is drifted along the unstable manifold of the periodic orbit and then strong chaos becomes apparent destabilizing the planetary system. The orbital elements start oscillating irregularly, whereas the resonant angles start to rotate, apart from $\Delta\Omega$, which shows very small libration around 180° , due to the conservation of the angular momentum. The planets show temporary

captures in different resonances and at the end of the evolution are found to be captured in 2/3 resonance (namely, planet P_2 became the inner planet) and $\Delta\varpi$ librates.

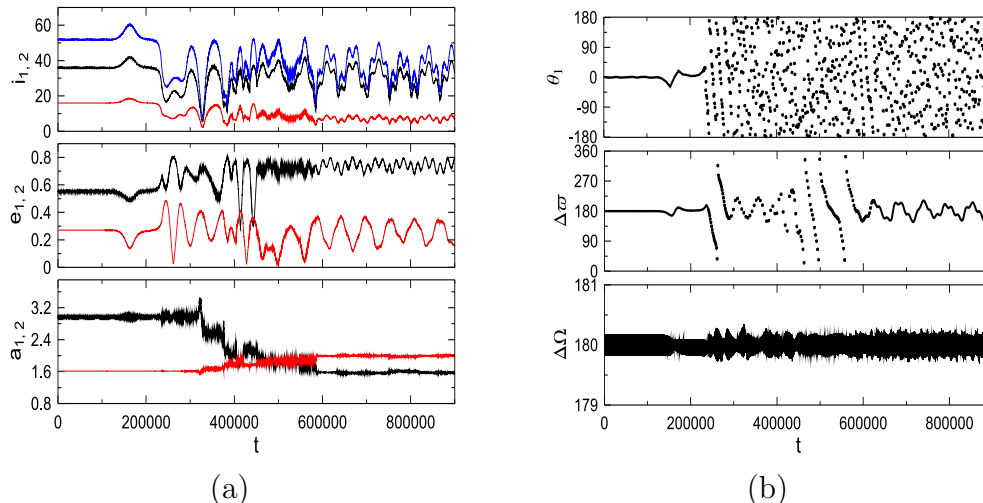


Figure 17: The evolution of orbital elements a_i , e_i , i_i , resonant angles θ_1 , $\Delta\varpi$ and $\Delta\Omega$ of a planetary system with initial conditions very close to an unstable periodic orbit (16). Red and black line stands for inner (P_1) and outer planet, P_2 , respectively. Blue line (in the top panel) stands for the mutual inclination Δ_i .

5.2 Case ii: Long-term evolution of a 3D stable orbit

We consider the stable periodic orbit:

$$\begin{aligned}
 a_1 &= 1.43, & e_1 &= 0.23, & i_1 &= 9.94^\circ, & \Omega_1 &= 90^\circ, & \omega_1 &= 270^\circ, & M_1 &= 0^\circ \\
 a_2 &= 2.64, & e_2 &= 0.56, & i_2 &= 22.13^\circ, & \Omega_2 &= 270^\circ, & \omega_2 &= 270^\circ, & M_2 &= 180^\circ
 \end{aligned}
 \tag{17}$$

During the evolution of the exact periodic orbit, the osculating elements and the resonant angles are almost constant and, approximately, equal to their initial values. However, if we consider orbits with initial conditions that deviate from the initial conditions of the stable periodic orbit, we should obtain quasiperiodic regular evolution. For instance, if we use the initial conditions (17), but set the initial ascending node of the outer planet $\Omega_2 = 280^\circ$, we obtain the evolution shown in Fig. 18. All orbital elements and the presented angles oscillate regularly around the initial values of the periodic orbit. So, an island of stability should exist around the orbit (17).

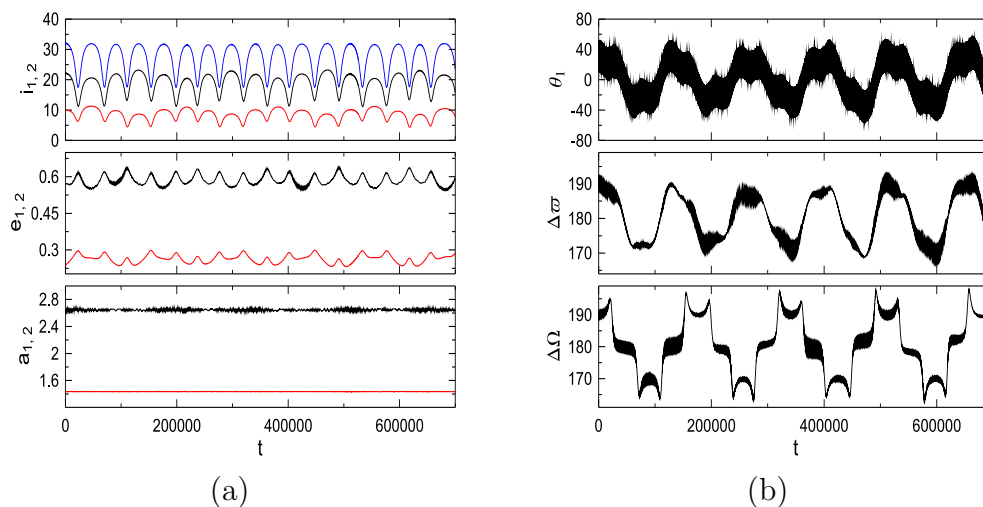


Figure 18: Long-term evolution of a planetary system with initial conditions as those of the stable periodic orbit (17) but with $\Omega_2 = 280^\circ$ (presentation as in Fig. 17).

If we do not start sufficiently close to the stable periodic orbit, i.e. if we increase the initial Ω_2 value by 14° with respect to the periodic orbit (17), we enter a chaotic region in phase space. The evolution is presented in Fig. 19. Until 10^4 t.u. the orbital elements and the presented angles librate around their expected values. Then, although $\Delta\varpi$ continues to librate, θ_1 rotates indicating that the system left the region around the periodic orbit. In the interval $9 - 9.3 \times 10^4$ close encounters between the planets take place. Then, slow rotation of the apsidal difference $\Delta\varpi$ is observed besides the rotation of θ_1 . Finally, we observe that the planet P_2 is scattered.

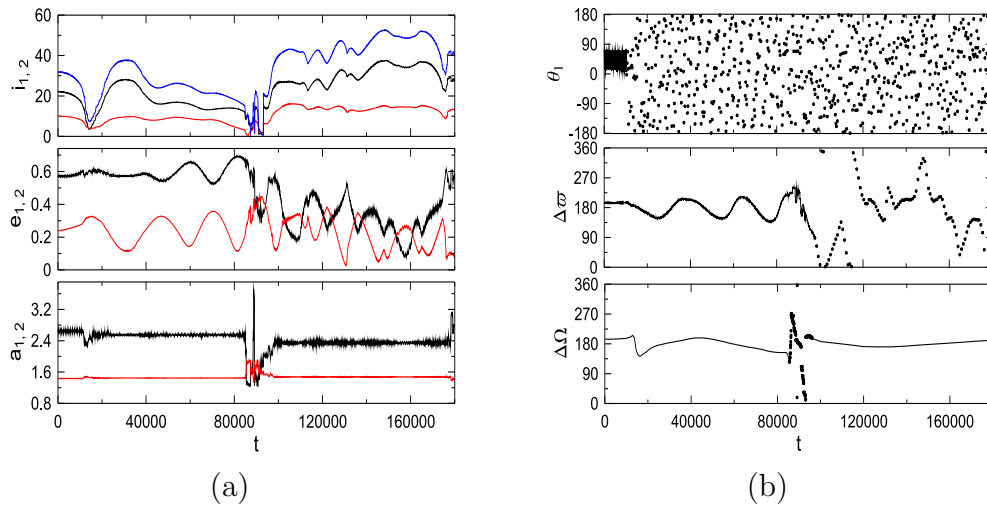


Figure 19: Long-term evolution of a planetary system with initial conditions as those of the stable periodic orbit (17) but with $\Omega_2 = 284^\circ$ (presentation as in Fig. 17).

6 Conclusions

Using the general three body problem as a model for the study of the dynamics of resonant planetary systems, we determined families of periodic orbits in the planar and spatial case and examined their stability. The orbital periodicity refers to a particular rotating frame for the model. Such periodic orbits indicate the exact mean motion resonances in phase space. We have performed an extensive study and provide results for $4/3$, $3/2$, $5/2$, $3/1$ and $4/1$ resonances.

In the planar problem, we presented the families of symmetric periodic orbits in the plane of eccentricities (e_1, e_2) for various values of planetary mass ratio. All symmetric periodic orbits can be classified in four different configurations, which are distinguished by the different values of the resonant angles (θ_1, θ_2) , namely we have the cases $(0, 0)$, $(0, \pi)$, $(\pi, 0)$ and (π, π) . In cases like 2nd order resonances the different configurations are distinguished by the pairs (θ_3, θ_1) . Some common features for all the examined resonances are the following:

- The majority of periodic orbits in the configuration (π, π) is unstable.
- In the configuration $(\pi, 0)$, we always obtain a phase protection mechanism and we have stable planetary orbits that cross each other.

- In the configuration $(0, \pi)$, we obtain families of stable periodic orbits that bifurcate from almost circular orbits (we remark that close to circular orbits, the configuration may change, however, the generated families consist of stable segments, whose majority of orbits belongs to the $(0, \pi)$ configuration).

We determined the vertical stability for all computed planar periodic orbits. Orbits that are critical with respect to their vertical stability (vertical critical orbits or, briefly, v.c.o.) are analytically continued to the third dimension and therefore, are bifurcation points of families of periodic orbits in the spatial model. V.c.o. can be found to any configuration, but in our study, no v.c.o. were found in (π, π) case. Also, they can be stable or unstable with respect to their horizontal stability. From unstable v.c.o., the analytic continuation always generates unstable spatial periodic orbits. From stable v.c.o., either stable, or unstable periodic orbits may bifurcate in space. Nevertheless, our computations showed that in most cases stable v.c.o generate stable families of periodic orbits. Certainly, the stability type can change along the families.

We computed and presented families of spatial periodic orbits for all studied resonances, which are symmetric with respect to either xz -plane or x -axis. Particularly, we are interested in families starting from stable v.c.o.. Following the analytic continuation of the planar v.c.o. we obtained that stability may extend up to quite large values of planetary mutual inclination (up to 50° - 60° in some cases). The majority of stable spatial periodic orbits is quite eccentric, because the corresponding v.c.o. are quite eccentric, too. An exception occurs for the $4/3$ resonance, where circular inclined orbits have been computed. Also, stable inclined orbits of low inclination values exist in $5/2$ resonance (families $F_{(0,\pi)}^{5/2}$), but with mutual inclination that does not exceed 12° .

Stable periodic orbits are associated with regions in phase space, where the majority of orbits evolves regularly twisting invariant tori. For initial conditions in such regions, a planetary system of two planets shows long-term stability and may, also, survive under small external perturbations (e.g. by additional planets in the system). In contrary, if a planetary system is positioned in the vicinity of an unstable periodic orbit, due to the existence of chaotic regions around it, it will eventually destabilize. This procedure could trigger irregular evolution that generally leads to close encounters between the planets and perhaps forces one planet to be scattered.

If, indeed, families of periodic orbits constitute paths that can drive the migration process of planets as we mentioned in the introduction, then a planetary system should be found, after resonant capture, in the vicinity of

a stable periodic orbit. Therefore, our study can help determine and understand the reasons why, the discovered multi-planet systems possess certain attributes.

Acknowledgments. This research has been co-financed by the European Union (European Social Fund - ESF) and Greek national funds through the Operational Program “Education and Lifelong Learning” of the National Strategic Reference Framework (NSRF) - Research Funding Program: Thales. Investing in knowledge society through the European Social Fund.

References

- G. Anglada-Escudé, P. Arriagada, S. S. Vogt, E. J. Rivera, R. P. Butler, J. D. Crane, S. A. Shectman, I. B. Thompson, D. Minniti, N. Haghighipour, B. D. Carter, C. G. Tinney, R. A. Wittenmyer, J. A. Bailey, S. J. O’Toole, H. R. A. Jones, and J. S. Jenkins. A Planetary System around the nearby M Dwarf GJ 667C with At Least One Super-Earth in Its Habitable Zone. *The Astrophysical Journal Letters*, 751:L16, May 2012.
- K. I. Antoniadou and G. Voyatzis. 2/1 resonant periodic orbits in three dimensional planetary systems. *Celestial Mechanics and Dynamical Astronomy*, 115:161–184, 2013.
- C. Beaugé, S. Ferraz-Mello, and T. A. Michtchenko. Extrasolar Planets in Mean-Motion Resonance: Apses Alignment and Asymmetric Stationary Solutions. *The Astrophysical Journal*, 593:1124–1133, August 2003.
- N. Callegari and Á. Rodríguez. Dynamics of rotation of super-Earths. *Celestial Mechanics and Dynamical Astronomy*, June 2013. doi: 10.1007/s10569-013-9496-5.
- G. Campanella. Treating dynamical stability as an observable: a 5:2 mean motion resonance configuration for the extrasolar system hd 181433. *Monthly Notices of the Royal Astronomical Society*, 418:1028–1038, December 2011.
- G. Campanella, R. P. Nelson, and C. B. Agnor. Possible scenarios for eccentricity evolution in the extrasolar planetary system hd 181433. *Monthly Notices of the Royal Astronomical Society*, 433:3190–3207, August 2013. doi: 10.1093/mnras/stt959.

- S. Ferraz-Mello, C. Beaugé, and T. A. Michtchenko. Evolution of migrating planet pairs in resonance. *Celestial Mechanics and Dynamical Astronomy*, 87:99–112, 2003.
- S. Ferraz-Mello, T. A. Michtchenko, and C. Beaugé. *Regular motions in extra-solar planetary systems*, page 255. Springer, January 2006.
- C. Froeschlé, E. Lega, and R. Gonczi. Fast lyapunov indicators. application to asteroidal motion. *Celestial Mechanics and Dynamical Astronomy*, 67: 41–62, 1997.
- Krzysztof Goździewski, Maciej Konacki, and Andrzej J. Maciejewski. Orbital configurations and dynamical stability of multiplanet systems around sun-like stars hd202206, 14herculis, hd37124, and hd108874. *The Astrophysical Journal*, 645(1):688, 2006.
- J. D. Hadjidemetriou. Symmetric and asymmetric librations in extrasolar planetary systems: a global view. *Celestial Mechanics and Dynamical Astronomy*, 95:225–244, 2006.
- J. D. Hadjidemetriou and G. Voyatzis. On the dynamics of extrasolar planetary systems under dissipation: Migration of planets. *Celestial Mechanics and Dynamical Astronomy*, 107:3–19, 2010.
- M. Hénon. Vertical stability of periodic orbits in the restricted problem. i. equal masses. *Astronomy and Astrophysics*, 28:415, 1973.
- S. Ichtiaroglou and M. Michalodimitrakis. Three-body problem - the existence of families of three-dimensional periodic orbits which bifurcate from planar periodic orbits. *Astronomy and Astrophysics*, 81:30–32, 1980.
- S. Ichtiaroglou, K. Katopodis, and M. Michalodimitrakis. On the continuation of periodic orbits in the three-body problem. *Astronomy and Astrophysics*, 70:531, 1978/11/1 1978.
- J. Laskar and A. C. M. Correia. Hd 60532, a planetary system in a 3:1 mean motion resonance. *Astronomy and Astrophysics*, 496:L5–L8, March 2009.
- M. H. Lee and S. J. Peale. Dynamics and origin of the 2:1 orbital resonances of the gj 876 planets. *The Astrophysical Journal*, 567:596–609, 2002.
- A.-S. Libert and J. Henrard. Analytical study of the proximity of exoplanetary systems to mean-motion resonances. *Astronomy and Astrophysics*, 461:759–763, January 2007.

- C. Lovis, D. Ségransan, M. Mayor, S. Udry, W. Benz, J.-L. Bertaux, F. Bouchy, A. C. M. Correia, J. Laskar, G. Lo Curto, C. Mordasini, F. Pepe, D. Queloz, and N. C. Santos. The harps search for southern extra-solar planets. xxviii. up to seven planets orbiting hd 10180: probing the architecture of low-mass planetary systems. *Astronomy and Astrophysics*, 528:A112, April 2011.
- C. Marchal. *The three-body problem*. Elsevier, Amsterdam, 1990.
- M. Michalodimitrakis. On the continuation of periodic orbits from the planar to the three-dimensional general three-body problem. *Celestial Mechanics*, 19:263–277, 1979/4/1 1979.
- T. A. Michtchenko, C. Beaugé, and S. Ferraz-Mello. Stationary orbits in resonant extrasolar planetary systems. *Celestial Mechanics and Dynamical Astronomy*, 94:411–432, 2006.
- A. Niedzielski, K. Godziewski, A. Wolszczan, M. Konacki, G. Nowak, and P. Zieliski. A planet in a 0.6 au orbit around the k0 giant hd 102272. *The Astrophysical Journal*, 693(1):276, 2009.
- D. Psychoyos and J. D. Hadjidemetriou. Dynamics of extrasolar systems at the 5/2 resonance: application to 47 UMa. In Z. Knežević and A. Milani, editors, *IAU Colloq. 197: Dynamics of Populations of Planetary Systems*, pages 55–62, February 2005.
- H. Rein, J. C. B. Papaloizou, and W. Kley. The dynamical origin of the multi-planetary system hd 45364. *Astronomy and Astrophysics*, 510:A4, January 2010.
- C. Skokos. On the stability of periodic orbits of high dimensional autonomous Hamiltonian systems. *Physica D Nonlinear Phenomena*, 159:155–179, November 2001.
- J. H. Steffen, D. C. Fabrycky, E. B. Ford, J. A. Carter, J.-M. Désert, F. Fressin, M. J. Holman, J. J. Lissauer, A. V. Moorhead, J. F. Rowe, D. Ragozzine, W. F. Welsh, N. M. Batalha, W. J. Borucki, L. A. Buchhave, S. Bryson, D. A. Caldwell, D. Charbonneau, D. R. Ciardi, W. D. Cochran, M. Endl, M. E. Everett, T. N. Gautier, R. L. Gilliland, F. R. Girouard, J. M. Jenkins, E. Horch, S. B. Howell, H. Isaacson, T. C. Klaus, D. G. Koch, D. W. Latham, J. Li, P. Lucas, P. J. MacQueen, G. W. Marcy, S. McCauliff, C. K. Middour, R. L. Morris, F. R. Mullally, S. N. Quinn, E. V. Quintana, A. Shporer, M. Still, P. Tenenbaum, S. E. Thompson,

- J. D. Twicken, and J. Van Cleve. Transit timing observations from kepler - iii. confirmation of four multiple planet systems by a fourier-domain study of anticorrelated transit timing variations. *Monthly Notices of the Royal Astronomical Society*, 421:2342–2354, April 2012.
- J. H. Steffen, D. C. Fabrycky, E. Agol, E. B. Ford, R. C. Morehead, W. D. Cochran, J. J. Lissauer, E. R. Adams, W. J. Borucki, S. Bryson, D. A. Caldwell, A. Dupree, J. M. Jenkins, P. Robertson, J. F. Rowe, S. Seader, S. Thompson, and J. D. Twicken. Transit timing observations from kepler - vii. confirmation of 27 planets in 13 multiplanet systems via transit timing variations and orbital stability. *Monthly Notices of the Royal Astronomical Society*, 428:1077–1087, January 2013.
- G. Voyatzis. Chaos, order, and periodic orbits in 3:1 resonant planetary dynamics. *The Astrophysical Journal*, 675:802–816, 2008.
- G. Voyatzis and J. D. Hadjidemetriou. Symmetric and asymmetric librations in planetary and satellite systems at the 2/1 resonance. *Celestial Mechanics and Dynamical Astronomy*, 93:263–294, 2005.
- G. Voyatzis, T. Kotoulas, and J. D. Hadjidemetriou. On the 2/1 resonant planetary dynamics - periodic orbits and dynamical stability. *Monthly Notices of the Royal Astronomical Society*, 395:2147–2156, 2009.
- R. A. Wittenmyer, J. Horner, and C. G. Tinney. Resonances required: Dynamical analysis of the 24 sex and hd 200964 planetary systems. *The Astrophysical Journal*, 761:165, December 2012.